# Relative Frequency Calibration for Fast Frequency Sweep Microwave Reflectometry

Akira EJIRI,  Yoshiyuki SHIMADA,  Takuma YAMADA[1],  Takuya OOSAKO,  Yuichi TAKASE
and  Hiroshi KASAHARA[2]

*Graduate School of Frontier Sciences, The University of Tokyo, Kashiwa 277-8561, Japan*
[1]*Research Institute for Applied Mechanics, Kyushu University, Kasuga 816-8580, Japan*
[2]*National Institute for Fusion Science, Toki 509-5292, Japan*

A frequency-modulated reflectometer with a frequency band of 26.5 to 40 GHz has been constructed and installed in the TST-2 spherical tokamak to measure fast density profile evolution. In order to calibrate the instantaneous frequency for various frequency sweep rates, a waveform matching method has been proposed and applied to the reflectometer. This method compares the interference patterns (i.e., waveforms) of a fixed target reflection, which do not depend on the sweep rate, and obtains the instantaneous frequency by fitting the target waveform time to the time for a reference sweep waveform. This allows evaluation of output frequency stability. The overall frequency error, including reproducibility, is around 0.1 GHz. Sweep rates up to 20 μs were used to measure the density profile evolution during rf heating.

## 1. Introduction

Microwave reflectometry launches microwaves into plasmas, and uses the reflection of the microwaves at a cutoff layer in the plasma. Since the phase of the reflected wave is a function of the optical distance, a density profile can be reconstructed from the phase, which is a function of the launched microwave frequency [1, 2]. Frequency-modulated (FM) microwave reflectometry is a density profile measurement method, and it is used widely in fusion plasma devices [3–9]. In this method, the frequency is swept periodically with a sawtooth-like waveform, using a function generator. The location of a given density can be calculated by the Abel inversion, where the group delay is integrated in microwave frequency from the frequency corresponding the plasma boundary (= 0 for O-mode) to that corresponding to the target location (i.e., cutoff). Therefore the location is a function of not only the phase for the corresponding microwave frequency, but also of phases below the microwave frequency.

When density fluctuations distort the phase data at a specific time (i.e., at a specific frequency), they affect the profile above the frequency. Therefore, the frequency sweep rate must be fast enough to take a snapshot profile.

The investigation on the effects of sweep period on the profile reconstruction in the GAMMA 10 mirror device revealed that for 12 to 18 GHz, a period less than 10-30 μs was necessary to obtain reliable profiles [5]. In addition, the required minimum sweep rate depended on the

phase calculation method. That study used a hyperabrupt varactor-tuned oscillator (HTO), which is a type of voltage controlled oscillators (VCOs). Both the VCO and the driving circuit have a finite time response. Thus, the controllability and the stability of output frequency should be evaluated for each system. For example, the system in reference [9] showed a time delay and hysteresis.

For a fast sweep rate, the microwave frequencies start to deviate from the expected values. Thus, it is important to evaluate the instantaneous microwave frequency during each sweep. Poor stability requires monitoring the frequency in each sweep. For slow sweeps analog or digital frequency measurement instruments can be used, but fast sweeps require faster measurements. One such method is mixing the microwave with the wave from a comb generator, which has a comb-shape frequency spectrum. When the microwave frequency is swept, the mixing output shows spikes at each frequency of the comb generator. The ASDEX-Upgrade reflectometer obtained 25 frequency points in this manner [8]. To obtain higher resolution (i.e., more frequency measurement points), interference patterns in a reference path dedicated for the frequency calibration were used. Phase evolution during a sweep is derived from the interference pattern using the Hilbert transform of the pattern. The interference pattern is also used in reference [9]. They used an in-phase and quadrature phase detector (i.e., demodulator), which enables direct phase extraction from the cosine and sine components of the interference. In these methods, instanta-

neous microwave frequencies were obtained by measuring the phase of the interference pattern; and the starting frequency was determined by another method.

This paper proposes a relative frequency calibration (i.e., measurement) method, which compares waveforms from a slow reference sweep and a fast target sweep, and evaluates the deformation of the target waveforms. The frequency of the slow reference sweep is obtained by another method, and for the target fast sweep, time for a given microwave frequency is obtained by matching the two waveforms. This method does not require the determination of the starting frequency, and the frequency accuracy depends on the accuracy of the waveform measurement. The method was used for the relative calibration of a reflectometer installed in the TST-2 spherical tokamak [10]. Sweep rates up to 50 kHz were used in the TST-2 density profile measurements, although the waveform matching method itself can be applied for faster sweep rates.

## 2. System Description

A microwave reflectometer with a frequency range of 26.5 to 40 GHz was designed and constructed to measure the density profile and fast density fluctuations induced by rf heating waves. A frequency sweepable source, using a voltage controlled oscillator (VCO) (SIVERSMA VO3260C/00), measured the density profile. The VCO produces a wave with a frequency range of 6.625 to 10 GHz, and the output frequency is multiplied by four using an active multiplier. An external voltage (5-25 V) controls the frequency of the VCO. The control voltage is produced by a function generator (Tektronix AFG3022) and amplified five times by a non-inverting amplifier, which uses an operational amplifier (National semiconductor LM6364). The instantaneous microwave frequency during a sweep should be measured or calibrated before operating the source at a very fast sweep rate. In addition, the stability and reproducibility of the frequency must be confirmed unless the frequency is calibrated during plasma measurements.

Figure 1 is the schematic drawing of the microwave reflectometer. The system is similar to conventional frequency-modulated (FM) reflectometers, however, it uses an in-phase and quadrature (IQ) demodulator to detect microwaves. The IQ-demodulator consists of two mixers and yields sine and cosine components of the microwave fed to the RF port. This is very useful for tracking the phase, and it obtains more unambiguous phase evolution than conventional FM systems, which uses a single mixer (or detector). Another different feature is that imaging optics generate a small illuminating spot at the cutoff layer. The optics are designed using the Kirchoff integral and consist of two concave mirrors, and the launching and receiving scalar horns [11].

The function generator supplies a sawtooth-like sweep
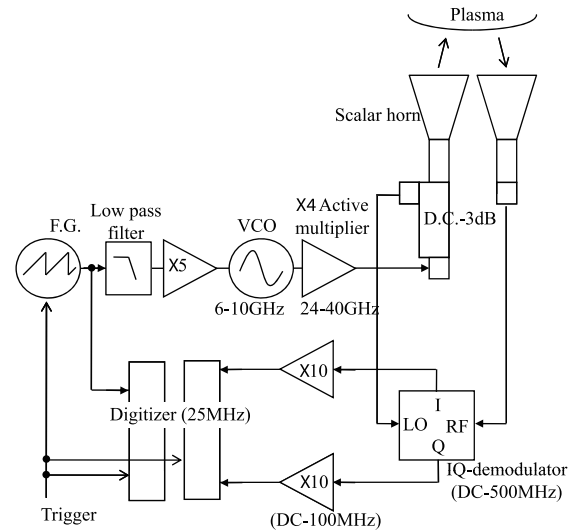


Fig. 1   Schematic drawing of the microwave reflectometer.
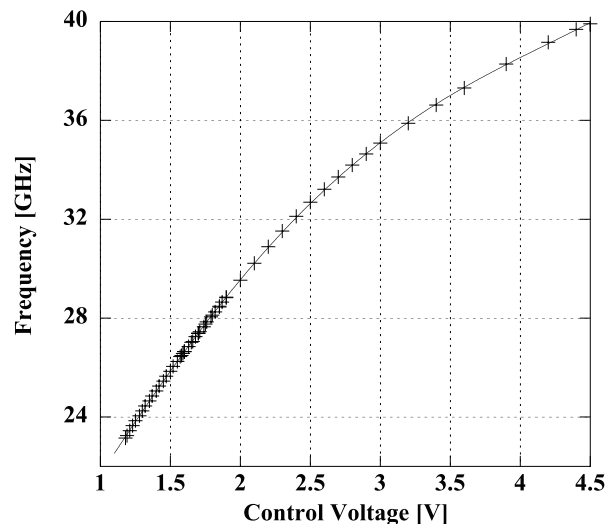


Fig. 2   Output microwave frequency as a function of the control voltage to the source part. Solid curve represents a polynomial fitting curve.

waveform that is low-pass filtered and multiplied by an amplifier to provide the VCO with a control voltage. The sweep waveform from the function generator is monitored by a fast digitizer with a sampling rate of 25 MHz. This monitor waveform is termed control voltage. The low-pass filter (RC = 0.01 μs) is necessary to reduce FM noise of the source, which is generated by a high power rf wave for plasma heating. The ×5 amplifier (DC–0.4 MHz) has a finite slew rate of around 300 V/μs, which produces additional delay.

Figure 2 shows the microwave output frequency as a function of the control voltage. This relationship is obtained by changing the voltage slowly, therefore, this relationship is static. The relationship for fast sweep operation is different, as discussed in Sec. 3. The frequency

is measured by a cavity-type frequency meter in the frequency range of 26.5 to 40 GHz. The data from the lower frequency range (< 26.5 GHz) is derived from the frequency difference between a Gunn oscillator with a fixed frequency and the VCO source. The frequency difference is obtained by measuring the mixing signal of both sources. A quartic polynomial function approximates the microwave frequency (see solid curve in Fig. 2). The overall frequency accuracy, including the fitting error and the frequency reproducibility of the source, is less than about 0.05 GHz for the static relationship.

The IQ-demodulator yields cosine and sine components of the reflected wave. These components are recorded by another fast digitizer which has two input channels called Ch. 1 and Ch. 2. The function generator and the digitizers are triggered just before each discharge. The function generator operates in burst mode to synchronize the sweep timings and other operational timings, such as the high-power rf wave injection. In burst mode, each trigger produces periodic sweep waveforms. Before a trigger, the generator yields a constant voltage. Burst mode operation and the finite system response produce a time dependent effect on the output microwave frequency discussed in Sec. 4.

## 3. Waveform Matching

This section describes the waveform matching method used to obtain the instantaneous microwave frequency by comparing the interference patterns for the fast target sweep and the slow reference sweep. We assume that the microwave frequency is deformed in time domain, and the resultant interference pattern is deformed only in the time space (i.e., in the horizontal direction), but not in the vertical direction. The validity of this assumption will be confirmed through the analysis. First, the frequency deformation is described, then the deformation of the interference pattern is described. Next, we compare the instantaneous frequencies for slow and fast swept cases. Waveforms for slow sweep (with a sweep period of 1 ms) and those for a fast sweep (with a sweep period of 0.02 ms) demonstrate the waveform matching method.

The microwave frequency from the VCO and active multiplier source is a function of the control voltage to the VCO. When the control voltage from a function generator $V$ is swept slow enough, the output microwave frequency is described by the static function $F(V)$ shown in Fig. 2. The function generator produces a time-dependent control voltage $V_T(t)$, where subscript $T$ represents the sweep period, and $t$ is the time normalized by $T$. For the slow sweep case, the instantaneous microwave frequency $f_{\text{slow}}(t)$ is a function only of $V$, and in this case,

$$f_{\text{slow}}(t) = F(V) = F(V_{\text{slow}}(t)), \tag{1}$$

where $V_{\text{slow}}(t)$ is the slow sweep waveform. However, when the sweep rate is fast, this relationship is not gener-

ally valid, even if $V_{\text{fast}}(t) = V_{\text{slow}}(t)$, where $V_{\text{fast}}(t)$ is the fast sweep waveform. Therefore, $f_{\text{fast}}(t) \neq F(V_{\text{fast}}(t))$, where $f_{\text{fast}}(t)$ is the instantaneous frequency. The difference arises from the finite (i.e., slow) responses of the function generator, the low-pass filter, the voltage amplifier, and the VCO itself. For a sawtooth-like frequency sweep, the resultant output microwave frequency shows a delay $\Delta$, which is defined as

$$f_{\text{slow}}(t - \Delta) = f_{\text{fast}}(t) , \tag{2}$$

here $\Delta$ is positive. This equation implies that the fast sweep frequency at a normalized time $t$ is equal to the slow sweep frequency at an earlier normalized time $t - \Delta$. When we obtain $\Delta$ using the waveform matching method, we obtain the instantaneous microwave frequency $f_{\text{fast}}(t)$. Generally, $\Delta$ is not a constant, but depends on the sweep rate for a given sweep waveform. Moreover, during a sweep, $\Delta$ changes with $t$ (i.e., frequency). Thus, we use the notation $\Delta_T(t)$.

When reflection occurs, the mixer outputs of the reflectometer $y_T(t)$ show interference patterns. For a fixed target, which is a square stainless plate in this case, the waveform is a function only of $f_T(t)$. Therefore, this waveform can serve as marker for the instantaneous microwave frequency $f_T(t)$. Figure 3 compares the control voltages $V_T(t)$ from the function generator and the waveforms of Ch. 1 of the IQ-demodulator for sweep periods of $T = 1$ ms and $T = 0.02$ ms. While the former signal shows a sharp sawtooth, the latter signal shows a dull waveform, caused by the finite response of the function
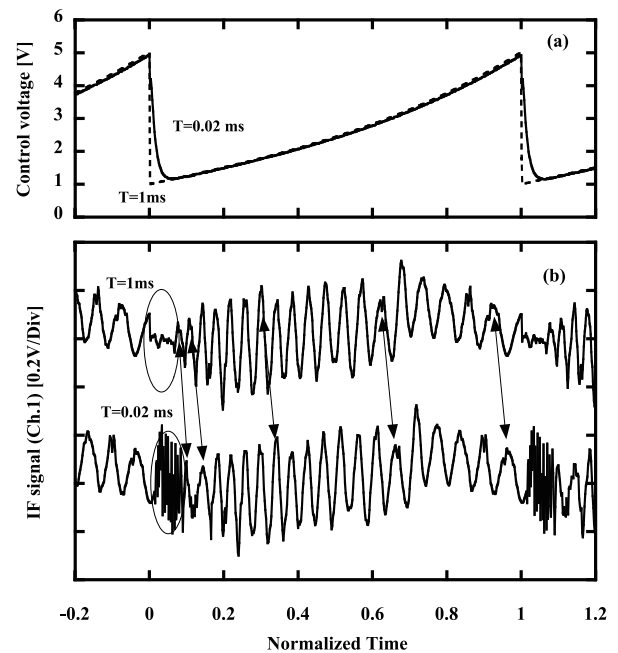


Fig. 3 Control voltages from the function generator (a) and the waveforms from Ch. 1 of the IQ-demodulator (b), as a function of the normalize time for sweep periods of $T = 1$ and $T = 0.02$ ms.

generator. Note that the horizontal axis represents the normalized time, and the origins are shifted so that the sawtooth tops occur at $t = 0$. Several sweep periods between $T = 1$ ms and $T = 0.001$ ms have been measured and analyzed by this method. The delay $\Delta_T$ decreased rapidly with $T$ and extrapolation indicates that $\Delta_{1\,\mathrm{ms}}$ is less than about 0.01 % corresponding to a frequency error of 0.002 GHz. Thus, $\Delta_{1\,\mathrm{ms}}$ is negligible and $T = 1$ ms satisfies Eq. (1) for the slow sweep. $T = 0.02$ ms corresponds to the fast sweep. Both interference patterns show almost the same waveform, except that the waveform for $T = 0.02$ ms was delayed compared with that for $T = 1$ ms (see arrows in Fig. 3 (b)). The delay is obvious in this case, although the differences in the control voltages are negligible during most of a period. The similarity between mixer outputs, including the fine structures, is almost perfect. At the early phase, however, delay differs from that in the later phase (see the leftmost arrow in Fig. 3 (b)). Therefore, the relationship between waveforms cannot be described by a simple constant delay, but can be represented by a delay $\Delta_T(t)$ as shown later. Since the mixer output $y_T(t)$ is a function only of the instantaneous microwave frequency $f_T(t)$, the output can be written by

$$y_{\mathrm{fast}}(t) = y_{\mathrm{slow}}(f_{\mathrm{fast}}(t)) = y_{\mathrm{slow}}(f_{\mathrm{slow}}(t - \Delta_T(t))) , \quad (3)$$

where Eq. (2) is used. $y_{\mathrm{slow}}(f)$ represents the static relationship between the frequency and the interference pattern. As long as the sweep waveform is fixed, $f_{\mathrm{slow}}(t)$ is only a function of $t$. The subscript $T$ in $\Delta_T(t)$ is the fast sweep period. Finally, we obtain the relationship

$$y_{\mathrm{fast}}(t) = y_{\mathrm{slow}}(t - \Delta_T(t)). \quad (4)$$

We use this relationship to obtain a parameterized $\Delta_T(t)$, whose parameters are determined through the fitting of $y_{\mathrm{fast}}$ to $y_{\mathrm{slow}}$. The initial rapid oscillating signal (see the bottom ellipse in Fig. 3 (b)), caused by a rapid frequency decrease, is excluded from the target time window in the fitting. In the example described below, we use the fitting function

$$\Delta_{T=0.02\,\mathrm{ms}}(t) = \sum_{i=0}^{5} a_i t^i + \frac{a_6}{t}, \quad (5)$$

where $a_0, \ldots, a_6$ are the fitting parameters. The analysis (target) time window was $0.14 < t < 1.007$ in this example. The term $1/t$ and a relatively higher order for the polynomial function are necessary to express the initial large deformation shown by the leftmost arrow in Fig. 3 (b). When we choose a narrower target time window, fewer parameters suffice. The fitting quality (i.e., agreement of the left- and right-hand sides of Eq. (4)) affects the validity of the assumption that the fast interference pattern is represented by a time delayed slow pattern.

Figure 4 compares the waveforms as a function of normalized time. The top trace represents the original fast sweep waveform from Ch. 1 of the mixer, which corresponds to $y_{\mathrm{fast}}(t)$ in Eq. (4). The second trace is the same
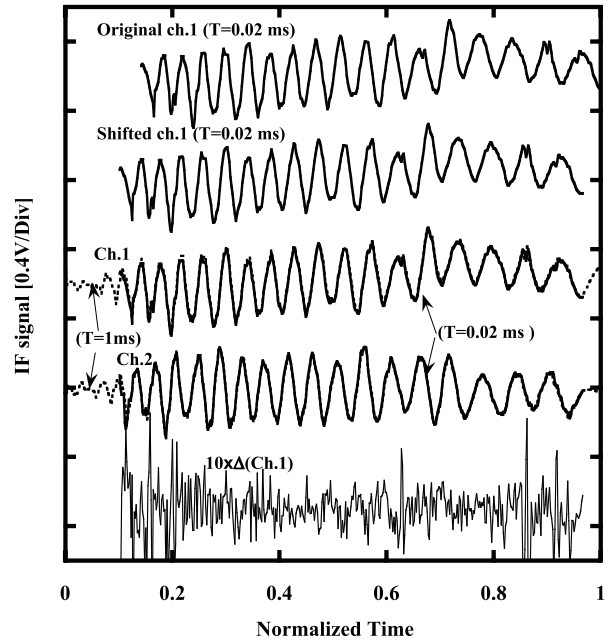


Fig. 4 Original Ch. 1 waveform, shifted Ch. 1 waveform, and fitting of Ch. 1 and Ch. 2 waveforms (solid curves) to the slow sweep waveforms (dotted curves). The bottom trace represents the residual fitting error, expanded 10 times on the vertical scale.

but shifted, which corresponds to $y_{\mathrm{fast}}(t + \Delta_{0.02\,\mathrm{ms}}(t))$. The third is the same as the second, but plotted over $y_{\mathrm{slow}}(t)$ with a sweep period of $T = 1$ ms. They are in very good agreement, not only in time, but also in amplitude, as shown by the bottom traces, which represent the residual fitting error ($y_{\mathrm{slow}}(t) - y_{\mathrm{fast}}(t + \Delta_{0.02\,\mathrm{ms}}(t))$) with an expanded vertical scale. The bottom traces for Ch. 2 also show good agreement. This implies that fast sweep operation deforms only the microwave frequency. Moreover, the agreement indicates that the mixer and the IF amplifier have very fast response times. Slow response smoothes out the waveforms and the method fails. In practice, rapid oscillation during the frequency decreasing phase of the sawtooth sweep, which is not used in the analysis, is smoothed out for $T = 0.02$ ms (see ellipses in Fig. 3 (b)).

Figure 5 (a) shows the delay $\Delta_{0.02\,\mathrm{ms}}(t)$ as a function of $t$ for three adjacent sweeps. In this case, $\Delta$ is around 4 %. The microwave frequency is about 0.8 GHz lower than expected from the control voltage (Fig. 5 (b)). The scatter of the three traces in the figure includes the effect of noise in the waveform matching method, and the reproducibility of the frequency sweep. The scatter is less than about 0.0005, which corresponds to a time scatter of 0.01 μs and a frequency scatter of about 0.01 GHz for the case $T = 0.02$ ms. The quick increase in $\Delta$ around $t \sim 0.2$ corresponds to the distortion around the leftmost arrow in Fig. 3 (b). The waveform matching method can be applied to a shorter sweep period such as $T = 0.01$ ms, but $T \sim 0.02$ ms is the present practical limit. For shorter

sweep periods, the (beat) frequency of the interference patterns in plasma measurements becomes too high for the digitizer.

Here we discuss the appropriate number of fitting parameters. In the cases presented in this section, we used seven fitting parameters in Eq. (5) to represent the frequency shift. However, it is not clear, whether the number of parameters suffices. More may be needed to obtain the required frequency accuracy. When we increase the number of fitting parameters, the residual error decreases, and fine structures appear in $\Delta_{0.02\,\mathrm{ms}}(t)$, but the fine structures change for different sweeps. Therefore, seven fitting parametes are enough to represent the systematic frequency shift. The residual fitting error (Fig. 4 bottom trace) can arise from random frequency shifts, and from errors in waveform measurement, such as amplifier noise. If we assume that the random frequency shifts are dominant, we can estimate the rms amplitude of the random frequency shifts from the rms amplitude of the residual error, which is about 0.1 GHz. When the random frequency shifts are dominant, the error should become large when the waveform crosses zero, and should decrease at the top and bottom of the waveform. The residual error seems independent of the waveform, however, and the above feature was not found. Thus, random frequency shifts are much smaller than our estimate, and the seven fitting parameters are enough to reproduce the frequency with an accuracy much smaller than 0.1 GHz. In the analysis of experimental data we used six fitting parameters, excluding the $1/x$ term, to represent the frequency. Our analysis

did not use the inital low frequency part, and $1/x$ term was not necessary.

Note that seven fitting parameters are required mainly to represent the initial quick change in $\Delta_{0.02\,\mathrm{ms}}(t)$, and the number can be reduced when we omit that initial part.

## 4. Stability of the Microwave Frequency

The practical accuracy of the instantaneous frequency is determined by the effects of several system components. The accuracy of the waveform matching method itself is very good, as described in the previous section. Here, using the waveform matching method, we will show the change in the time delay, which reflects the stability and reproducibility of the microwave frequency.

In order to compare the overall features of the different sweeps, we use a single constant delay (i.e., one fitting parameter) and a narrower time window ($0.2 < t < 1.0$), rather than the seven fitting parameters and wider time window ($0.14 < t < 1.007$) used in the previous section. Figure 6 shows the delay $\Delta$ as a function of the time from a trigger. Six traces, obtained on three different days, are plotted using different symbols for the different days. Two different digitizers, in internal clock mode, were used for four traces (solid and dotted); and a single digitizer was used for the other two traces (dashed). $\Delta$ decreases quickly in the early period ($t < 1$ ms), and then increases linearly with time for four traces (solid and dotted). The former quick decrease has an exponential time constant of around 0.3 ms. Since the function generator produces sawtooth sweeps after a trigger, it takes a finite amount of time for
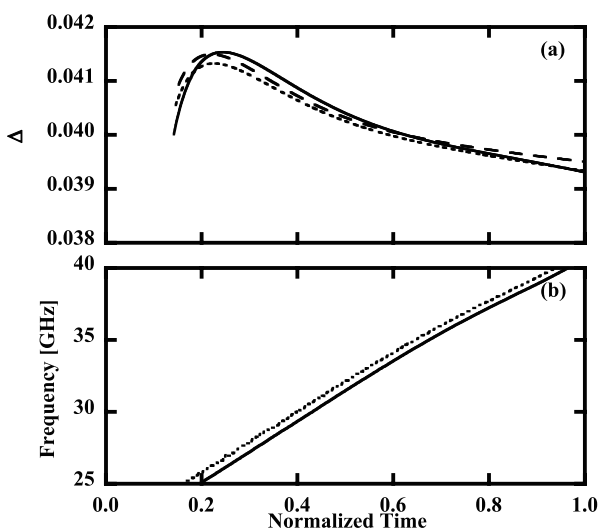


Fig. 5 Delay $\Delta_{0.02\,\mathrm{ms}}$ (a) and obtained frequency (solid curve) (b) as a function of $t$. Three $\Delta$s for three adjacent sweeps (solid, dashed and dotted curves) are plotted in (a). The solid curve in (b) represents the frequency corresponding the solid curve in (a). The dotted curve in (b) represents the frequency assuming a static relationship between the control voltage and the frequency.
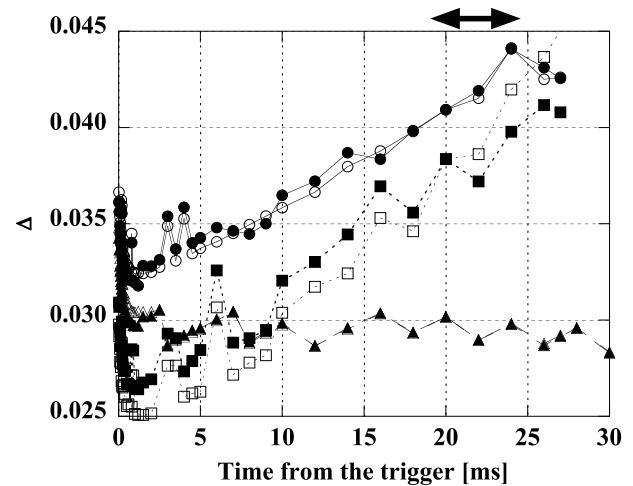


Fig. 6 Delay $\Delta$ as a function of time from a trigger. Different line styles represent measurements on different days. Traces with solid and dotted line styles were obtained using two digitizers with internal clocks, while the dasheded lines with triangles were obtained using one digitizer. Different symbols represent differences in the reference sweep.

the components to become completely periodic. The low-pass filter, the ×5 amplifier, and the VCO itself, can contribute to the initial rapid decrease. The traces with dashed lines were obtained with one digitizer, and the linear increase in Δ was not observed, while it was observed for traces obtained using two different digitizers. Therefore, the linear increase in Δ for the four traces (solid and dotted) is caused by a small difference in the sampling rates of the two digitizers (one is used for mixer outputs and the other monitors the control voltage). About $10^{-5}$ (i.e., 0.001 %) difference in the sampling rates causes expanding time difference, and results in a linear increase in Δ.

Different line styles in Fig. 6 represent measurements on different days, demonstarating that it is better to perform the calibration on the same day as the plasma measurements. The raw waveforms also show slight differences in their fine structures. Different symbols represent the difference in the reference sweep with a period of ($T = 1$ ms). Open symbols represent the data using the same reference sweep, while closed symbols represent the data using different reference sweeps. The small differences indicate that the reference (i.e., slowly sweep) frequency is stable. The height of the spikes in the curves corresponds to one or two sampling times (1, 2 × 40 ns). This can be attributed to the quantization of the time shift in the fitting, and the quantization leads to the spikes. The data with dotted curves show larger scatter than those with solid curves. During the former measurements, the stainless steel reflection target was reset between the slow and fast sweep measurements (i.e., calibration). The target was fixed during the measurement shown by solid and dashed curves. The larger data scatter probably reflects error in the target positioning. The horizontal arrow (from 19 to 24 ms) indicates a typical time window of the density profile measurements. Minimizing the microwave frequency error requires frequent calibration, and the resultant error is about 0.005, which corresponds to about 0.1 GHz. For slower sweep rates, Δ and its error decrease, although the static error ($\sim 0.05$ GHz) in the frequency curve (Fig. 2) remains.

In conclusion, the instantaneous microwave frequency can be derived with an error of about 0.1 GHz for a sweep period of 0.02 ms. The waveform matching method provides a tool for evaluating the error and stability of the microwave frequency, which are affected by various elements, including the finite responses of the components, and the accuracy of the reference target positioning.

## 5. Profile Measurements

Using the waveform matching method, microwave frequencies can be evaluated within the error bars of about 0.1 GHz. The error seems to be negligible, compared with other effects such as profile assumption at the edge and discharge reproducibility. The density profile of TST-2 plasmas was measured using the reflectometer. TST-2 is a

spherical tokamak with the following parameters [10]: major radius $R \leq 0.38$ m, minor radius $a \leq 0.25$ m, aspect ratio $A = R/a \geq 1.5$, elongation $\kappa \leq 1.8$, toroidal magnetic field $B_t \leq 0.3$ T, and plasma current $I_p \leq 0.14$ MA.

The reflectometer launches microwave with O-mode polarization. Figure 7 shows an example of TST-2 discharges where high-power rf heating was applied from $t = 20$ to 21 ms. Figure 8 shows the density profile evolution. In this case, the microwave frequency was swept with a period of 0.02 ms, and several profiles are shown in the figure. The first profile represents the point just before rf heating and the last profile represents that just after rf heating. These show that the density increases during heating. We applied the control voltage beyond its specified range,
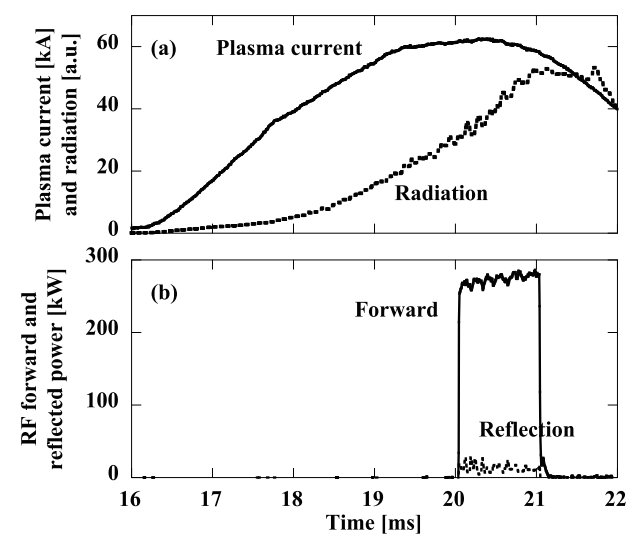


Fig. 7  Time evolutions of the plasma current and the radiation (a), and the forward and reflected rf power (b).
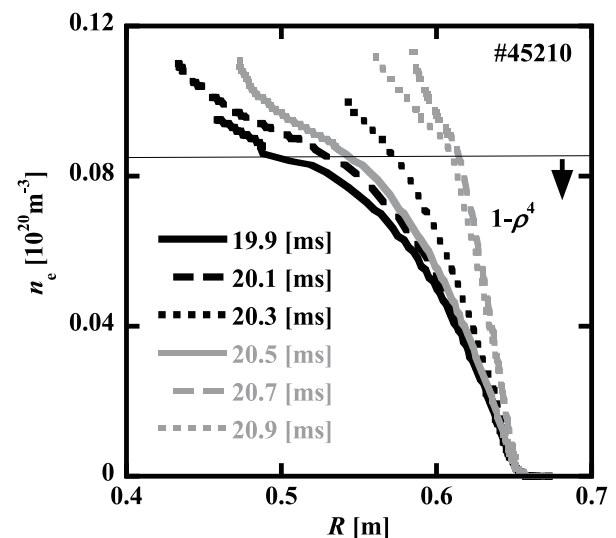


Fig. 8  Time evolutions of the electron density profile during rf heating.

and the lower frequency range ($< 26.5$ GHz) is out of the design range of the microwave source. Frequencies below 26.5 GHz suffered from a large source noise. Therefore, the frequency range above 26.5 GHz was used for profile reconstruction. The edge density profile corresponding to the frequency range below 26.5 GHz was assumed to have a shape. In this case, we assume a profile shape of $1 - \rho^4$, where $\rho$ is a normalized radius. Such an assumption for the edge density profile is necessary for reflectometry using O-mode polarization [12, 13]. The density increase resulting from the rf heating seems related to the degree of the absorption of the wave. The absorption is expected to increase for higher initial density and for stronger vertical field; in these cases, the density increase is less. High frequency density fluctuations can be measured by our reflectometer using a fixed frequency source. Spectra representing parametric decay instabilities were observed by the reflectometer and by magnetic pickup coils, when the absorption was expected to be poor [14].

## 6. Summary

For FM reflectometers, it is important to calibrate the instantaneous microwave frequency during the sweep. For this purpose, we propose a waveform matching method that compares the interference patterns (i.e., waveforms) of a fixed target reflection, obtaining the instantaneous frequency by fitting the time for the target waveform to the time for a slow sweep waveform. We applied this method to the reflectometer installed in the TST-2 spherical tokamak, and preformed frequency calibration for sweep rates down to 10 μs. This method can evaluate the stability of the output frequency, and we detrmined the finite response time in the microwave source and the slight differences in the sampling times of different digitizers, causing deviations of the microwave frequency from the ideal case. The overall frequency error, including the reproducibility,

is around 0.1 GHz, and once-a-day calibration is recommended to achieve this accuracy, as shown in Fig. 6. Sweep rates up to 20 μs were used to measure the density profile evolution during rf heating.

[1] F. Simonet, Rev. Sci. Instrum. **56**, 664 (1985).
[2] C. Laviron, A.J.H. Donne, M.E. Manso and J. Sanchez, Plasma Phys. Control. Fusion **38**, 905 (1996).
[3] F. Wagner *et al.*, *Plasma Phys. Controlled Nuclear Fusion Research 1990* (IAEA, Vienna, 1991) Vol.1 p. 277–290. M.E. Manso *et al.*, *18th Europ. Conf. on Contr. Fusion and Plasma Phys.* Berlin, **15C**, I-393 (1991).
[4] E.J. Doyle, Rev. Sci. Instrum. **61**, 2896 (1990).
[5] T. Tokuzawa *et al.*, Rev. Sci. Instrum. **68**, 443 (1997).
[6] F. Clairet *et al.*, Rev. Sci. Instrum. **72**, 340 (2001).
[7] K.W. Kim *et al.*, Rev. Sci. Instrum. **66**, 1229 (1995).
[8] A. Silva, P. Varela, L. Cupido, M. Manso, L. Meneses, L. Guimarais, G. Conway, F. Serra and the ASDEX Upgrade Team, *Proc. 7th Intl. Reflectometry. WS. IRW7* (Garching, 2005), IPP Report **II/9**, p. 3 (2005). URL: http://www.aug.ipp.mpg.de/IRW/IRW7/proceedings.html.
[9] S.-H. Seo and D.J. Lee, Rev. Sci. Instrum. **77**, 045103 (2006).
[10] Y. Takase *et al.*, Nucl. Fusion **41**, 1543 (2001).
[11] T. Yamada *et al.*, *to be published in* Plasma Fusion Res., in *Proc. of 16th International Toki Conference* (Toki, Japan, December 5–8, 2006).
[12] Y. Yokota, A. Mase, Y. Kogi, T. Tokuzawa and K. Kawahata, Plasma Fusion Res. **1**, 040 (2006).
[13] P. Varela, M.E. Manso, A. Silva, J. Fernandes and F. Silva, Rev. Sci. Instrum. **66**, 4937 (1995).
[14] T. Yamada *et al.*, Rev. Sci. Instrum. **78**, 083502 (2007).